Timing Modeling and Optimization Under the Transmission Line Model

Tai-Chen Chen, Song-Ra Pan, and Yao-Wen Chang, *Member*, *IEEE*

Abstract— **As the operating frequency increases to Giga Hertz and the rise time of a signal is less than or comparable to the time-of-flight delay of a wire, it is necessary to consider the transmission line behavior for delay computation. We present in this paper an analytical formula for the delay computation under the transmission line model. Extensive simulations with SPICE show the high fidelity of the formula. Compared with previous works, our model leads to smaller average errors in delay estimation. Based on this formula, we show the property that the minimum delay for a transmission line with reflection occurs when the number of round trips is minimized (i.e., equals one). Besides, we show that the delay of a circuit path is a posynomial function in wire and buffer sizes, implying that a local optimum is equal to the global optimum. Thus, we can apply any efficient search algorithm such as the well-known gradient search procedure to compute the globally optimal solution. Experimental results show that simultaneous wire and buffer sizing is very effective for performance optimization under the transmission line model.**

I. Introduction

As the operating frequency increases to Giga Hertz, the rise time of a signal is less than or comparable to the time-of-flight delay of a wire. Also, the die size is getting larger, resulting in longer global interconnection lines. The trends make it important to consider the transmission line behavior for delay computation [1]. Transmission line effects become significant when $t_r < 2\ t_f$, where t_r is the rise time and t_f is the time of flight determined by the wire length l divided by the velocity v [1]. There are two kinds of transmission lines. A wire with negligible resistance is called a *lossless transmission line*. However, on-chip interconnections have significant resistance, and they should be treated as *lossy transmission lines* [1], [6], [19]. Obviously, it is more accurate and desirable to consider line resistance for timing estimation and optimization. In this paper, therefore, we shall focus on lossy transmission lines.

When two transmission lines on a chip are connected and these two wires have different characteristic impedance, such mismatches of wire impedance can cause reflections at the junction point [1], [13]. Since reflections may cause logic failure or increase delay, the discontinuities of impedance at junction points must be controlled in order to minimize the side effect of reflections. On one hand, if the driving resistance is larger than the wire impedance, it requires multiple trips (a trip is a signal travels from one end of a line to the other end) to switch on the load; on the other hand, if the driving resistance is smaller than the wire impedance, the load may be falsely triggered. We can eliminate the reflections by matching the driving resistance and the wire impedance. The driving resistance of a gate and the impedance of a wire are approximately in inverse proportion to its size and width, respectively. Hence, wire and gate sizing can affect the delay, implying that sizing circuit components (wires and buffers) is applicable to delay optimization.

Manuscript received April 7, 2002; revised January 30, 2003. This paper was recommended by Editor-in-Chief Nagarajan Ranganathan.

This work was supported in part by the National Science Council of Taiwan ROC by Grant No. NSC-91-2215-E-002-036.

Tai-Chen Chen is with the Graduate Institute of Electronics Engineering, National Taiwan University, Taipei 106, Taiwan. E-mail: d90943008@ee.ntu.edu.tw.

Song-Ra Pan is with Taiwan Semiconductor Manufacturing Company, Ltd., Hsinchu 300, Taiwan. E-mail: gis87528@cis.nctu.edu.tw.

Yao-Wen Chang is with Department of Electrical Engineering & Graduate Institute of Electronics Engineering, National Taiwan University, Taipei 106, Taiwan. E-mail: ywchang@cc.ee.ntu.edu.tw.

A. Previous Work

Timing is a crucial concern in high-performance circuits. Many techniques such as wire sizing and gate sizing have been proposed to optimize timing (e.g., [3], [4], [5], [12], etc); however, most of the techniques are based on the Elmore delay model [8]. Modeling and analysis techniques for simulation and timing optimization under the lossy transmission line model have been studied extensively in the literature [9], [10], [11], [14], [17], [18], [21], [24], [26], [27], [28], [29], [30]. Previous work in [17] and [21] proposed precise methods for simulating waveform, but they did not present any delay estimator. The work in [18] and [28] modeled the transmission line effect; they, however, did not consider delay optimization. Several works in the literature consider the minimization of delay under the transmission line model. Gao and Wong in [9] and [10] applied continuous wire-sizing to minimize delay under the lossy transmission line model; however, they focused on exponentially tapered wires. Ismail and Friedman in [11] computed a uniform buffer size and the number of buffers to optimize the delay of a circuit path under the lossy transmission line model; however, their formula does not handle wire sizing. Lin and Pileggi in [14] proposed a wire sizing formulation with second order central moments, but their wire sizing formulation under the transmission line model is not always a posynomial program, and thus there is no optimality guarantee. The work in [26] and [30] adopted the S-parameter macro delay model to minimize delay and skew, but the sensitivities were computed at each step using finite difference approximation which requires expensive computation. The work in [24], [27], and [29] adopted higher order moments to minimize delay, but their delay models were computationally expensive.

B. Our Contribution

In this paper, we focus on delay modeling and timing optimization under the transmission line model. Unlike most previous works that are based on relatively complicated models (e.g., [17], [18], [27], and [28]) or incur larger errors (e.g., [8] and [11]), we present a simple, yet accurate formula for the delay computation under the lossy transmission line model. Extensive simulations with SPICE show that the formula has high fidelity, with an average error of within 5.93% for lossy transmission lines. Based on this formula, we show the property that the minimum delay for a lossy transmission line with reflection occurs when the number of round trips is minimized (i.e., equals one). Besides, we show that the delay of a circuit path is a posynomial function in wire and buffer sizes, implying that a local optimum is equal to the global optimum. Thus we can apply any efficient search algorithm, such as the well-known gradient search procedure, to compute the optimal wire and buffer sizes for timing optimization for a circuit path. For a routing tree (a routing tree is a tree that interconnects all signal terminals of a net), we propose a two-stage algorithm to optimize the delay. In the first stage, we traverse the tree to determine its critical path and delay. In the second stage, we control the reflections at all branching points to prevent from falsely triggering receivers and minimize the critical path delay. We repeat the two stages until no further improvements in the delay of the tree. Experimental results show that simultaneous wire and buffer sizing is very effective in minimizing the delays of circuit paths under the transmission line model.

The remainder of this paper is organized as follows. Section II introduces some notation. Section III gives the gate and the transmission line models. Section IV formulates the problem. Section V considers the simultaneous wire and buffer sizing for delay optimization. Section VI extends the cases on a general routing tree. Section VII shows the experimental results, and finally concluding remarks are given in Section VIII.

II. Notation

We use the following notation in this paper.

- $\hat{r}_b$: the resistance of a gate with unit size.
- r_i^b: the resistance of gate i.
- $\hat{c}_b$: the capacitance of a gate with unit size.
- c_i^b: the capacitance of gate i.
- g_i: the size of gate i.
- $\hat{c}_w$: the capacitance of a wire with unit size.
- $\hat{u}_w$: the inductance of a wire with unit size.
- $\hat{r}_w$: the sheet resistance of a wire.
- w_i: the width of wire i.
- l_i: the length of wire i.
- Z_i: the characteristic impedance of wire i.
- v_i: the propagation velocity of wire i.
- R_s: the driver resistance.
- C_L: the load capacitance.
- V_{DD}: the high voltage of power supply.
- V_{IH}: the minimum voltage at the input of a logic gate required so that gate switches.
- $\alpha_{i,j}$: the transmission coefficient at point i if a signal is transmitted from point i to point j.
- $\beta_{i,j}$: the reflection coefficient at point i if a reflection travels from point i to point j.
- γ_i: the voltage attenuation coefficient on wire i if a signal is transmitted from its source to sink.

III. Transmission Line Model

In this section, we give the wire and gate models, and discuss the transmission line effects which is importance when $t_r < 2\ t_f$, where t_r is the rise time and t_f is the time of flight determined by the wire length l divided by the velocity v [1].

A. Gate and Wire Modeling

Figure 1 illustrates the gate and the lossy transmission line models used in this paper. For a gate i with size g_i, the gate resistance r_i^b is $\hat{r}_b/g_i$ and the gate capacitance c_i^b is $\hat{c}_b g_i$, where $\hat{r}_b$ and $\hat{c}_b$ are the unit-sized resistance and unit-sized capacitance of a gate, respectively.

A uniform lossy transmission line i of width w_i can be represented by a serial sections of unit-length resistance, $\hat{r}_w/w_i$, unit-length inductance, $\hat{u}_w/w_i$, and unit-length capacitance, $\hat{c}_w w_i$, where $\hat{r}_w$, $\hat{u}_w$, and $\hat{c}_w$ are the sheet resistance, the unit-sized inductance, and the unit-sized capacitance of a wire, respectively. The effect of inductance and capacitance can be represented by a characteristic impedance, Z_i, which equals $\sqrt{(\hat{u}_w/w_i)/(\hat{c}_w w_i)} = \sqrt{\hat{u}_w}/(w_i\sqrt{\hat{c}_w})$. The propagation velocity of a wire i, v_i, equals $1/\sqrt{\hat{u}_w \hat{c}_w}$ [1]. If the length of a wire is l_i, its total resistance, total inductance, and total capacitance are $\hat{r}_w l_i/w_i$, $\hat{u}_w l_i/w_i$, and $\hat{c}_w w_i l_i$, respectively.

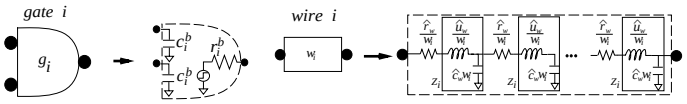

Fig. 1. A gate is the loading of its upstream, but is the driver of its downstream. A lossy transmission line is represented by a serial sections of its resistance, inductance, and capacitance, or we can merge each section of inductance and capacitance into a characteristic impedance.

Therefore, with the gate and the lossy transmission line models, we can represent a circuit path by resistors, capacitors, and characteristic impedance. Figure 2 illustrates the resulting circuit modeling for a circuit path with n buffers, where R_S and C_L are the driver resistance and the load capacitance, respectively.

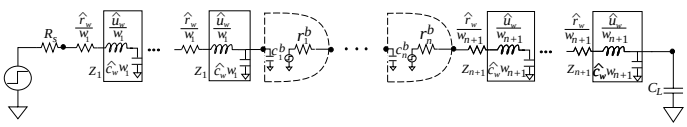

Fig. 2. A circuit path (with lossy transmission lines) is a combination of resistors, capacitors, and characteristic impedances.

B. Reflections on a Wire

Due to the inductive and capacitive discontinuities, the resulting reflections may cause logic failure or excessively longer delay [1], [13]. As shown in Figure 3, gate $i-1$ drives lossy transmission line i and gate i. Inductive and capacitive discontinuities may occur at the points A and B. The initial voltage at the point B is the sum of the signal sent out from the point A and the reflection generated at the point B. When the reflection generated at the point B travels backward to the point A, a new reflection generated at the point A is transmitted toward to the point B. The new voltage at the point B is the sum of the incoming reflection, the new outgoing reflection, and the initial voltage.

On one hand, as shown in Figure 4(a), if the resistance of the gate $i-1$, r^b_{i-1}, is larger than the impedance of the wire i, Z_i, the initial voltage at point B might not reach the threshold voltage. Thus, multiple round trips along the wire may be required to correctly transmit a signal. On the other hand, as shown in Figure 4(b), if r^b_{i-1} is smaller than Z_i, a reflection generated at point A is negative since the reflection coefficient $\beta_{i-1,i} = (r^b_{i-1} - Z_i)/(r^b_{i-1} + Z_i)$ is negative. Therefore, the voltage may oscillate at the point B, causing *overshoot* or *undershoot*. This oscillating pattern is called *ringing*. If r^b_{i-1} matches with Z_i, the source reflection coefficient $\beta_{i-1,i} = 0$. Thus, no reflections are generated at the source end A.

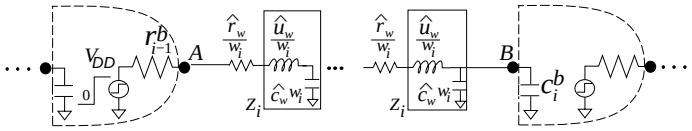

Fig. 3. The resistor with resistance r^b_{i-1} drives a lossy transmission line with characteristic impedance Z_i and a capacitor with capacitance c^b_i.

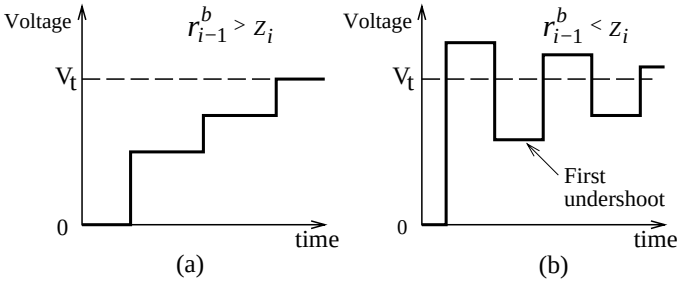

Fig. 4. (a) Multiple round trips are required to correctly transmit a signal. (b) Ringing may cause logic failures.

C. Voltage Attenuation on a Wire

In a lossy transmission line, the resistance of a wire causes voltage attenuation, and the voltage attenuation coefficient γ_i along a lossy transmission line i is derived in [1] as follows:

$$\gamma_i = e^{-\frac{\left(\frac{\hat{r}_w l_i}{w_i}\right)}{2 Z_i}} = e^{-\frac{\hat{r}_w l_i \sqrt{\hat{c}_w}}{2\sqrt{\hat{u}_w}}}. \quad (1)$$

Therefore, in Figure 3, the voltage at the point B before reflection is given by

$$V_B = \gamma_i V_A. \quad (2)$$

D. When to Use Transmission Line Analysis

According to [1], [15], and [22], the transmission line behavior is significant when

$$t_r < 2\, t_f, \quad (3)$$

and

$$Rl \leq 2\, Z_0, \quad (4)$$

where $t_r = 2.2\, r^b_{i-1}(\hat{c}_w w_i l_i + c^b_i)$ is the rise time of wire i, $t_f = l_i/v_i$ is the time-of-flight delay, $Rl = \hat{r}_w l_i / w_i$ is the total resistance, and $Z_0 = Z_i$ is the characteristic impedance. As illustrated in Figure 3, we can rewrite Inequalities (3) and (4) as Inequalities (5) and (6) as follows:

$$2.2\, r^b_{i-1}(\hat{c}_w w_i l_i + c^b_i) < 2\, \frac{l_i}{v_i}, \quad (5)$$

and

$$\frac{\hat{r}_w l_i}{w_i} \leq 2\, Z_i. \quad (6)$$

Besides, to make the voltage at the point B correctly drive the gate i, the voltage at the point B after infinite reflections should be greater than or equal to V_{IH}. In other words, the following inequality must be satisfied.

$$\begin{aligned} V_B &= 2\,\alpha_{i-1,i}\gamma_i(1 + \gamma_i^2\beta_{i-1,i} + \gamma_i^4\beta_{i-1,i}^2 + \ldots)V_{DD} \\ &= \frac{2\,\alpha_{i-1,i}\gamma_i V_{DD}}{1 - \gamma_i^2\beta_{i-1,i}} \\ &\geq V_{IH}, \end{aligned} \quad (7)$$

where

$$\begin{aligned} \alpha_{i-1,i} &= \frac{Z_i}{r^b_{i-1} + Z_i} \\ \beta_{i-1,i} &= \frac{r^b_{i-1} - Z_i}{r^b_{i-1} + Z_i} \\ \gamma_i &= e^{-\frac{\hat{r}_w l_i \sqrt{\hat{c}_w}}{2\sqrt{\hat{u}_w}}}. \end{aligned}$$

Therefore, we should model a wire as a lossy transmission line if Inequalities (5)–(7) are satisfied; it should be modeled as a distributed RC line, otherwise.

Note that, Inequality (5) can be reduced as follows by discarding c^b_i:

$$\begin{aligned} r^b_{i-1} &< \frac{2}{2.2\hat{c}_w w_i v_i} \\ &< Z_i. \end{aligned} \quad (8)$$

Since $r^b_{i-1} < Z_i$, ringing occurs (see Figure 4(b)). If ringing occurs, we may need to model a wire as a transmission line; it should be modeled as a distributed RC line, otherwise.

E. Delay Model

In this subsection, we introduce our delay model. Our delay model is based on the RC model. However, since the resistive loss causes voltage attenuation on a wire and the discontinuity of impedance at a junction point incurs reflection, we need to modify the original RC model. First, as given in Equation (1), the voltage attenuation coefficient γ_i along a lossy transmission line is less than 1 because the exponent of e is negative. Therefore, the *effective* resistance is not equal to the total resistance of the wire, implying that the pull-up resistance needs to be modified. Second, due to voltage attenuation and reflection, the final voltage may not equal V_{DD}, implying that we need to use an approximate method to correct the delay model. Third, due to reflection, multiple round trips may be required to correctly transmit a signal, implying that the number of round trips be considered in delay model. We describe in detail how to modify the original RC model in the following.

The time for charging the capacitive load (defined at 50% of the final value) of the lumped network equals $\ln 2 R_p C_L$, where R_p is the pull-up resistance and C_L is the total capacitive load [19], [20], [25]. According to [1], the current that a lossless transmission line can supply is limited by its characteristic impedance. As a result, looking from the receiving end, the line behaves like a resistor with a value Z_0. In a lossy transmission line, not only its characteristic impedance, but also its *effective* resistance supplies the current. If the total resistance of a wire causes voltage attenuation, the voltage at the receiving end becomes zero and the *effective* resistance equals the total resistance. In Section III-C, we know that the voltage at the receiving end V_B equals $\gamma_i V_A$. This implies that there is only $(1-\gamma_i)$ percentage of the total resistance for the line between nodes A and B, $\hat{r}_w l_i / w_i$, causing voltage attenuation and supplying current.

Consequently, the pull-up resistance R_p for the transmission line is equal to the sum of the characteristic impedance of the line, and partial resistance of the wire which causes voltage attenuation. We have the pull-up resistance R_p for the line as follows:

$$R_p = Z_i + (1-\gamma_i)\frac{\hat{r}_w l_i}{w_i}. \quad (9)$$

Hence, the time t_c for charging the capacitive load (at 50% of the voltage of the first overshoot) of a transmission line is given by

$$t_c = \ln 2 \left(Z_i + (1-\gamma_i)\frac{\hat{r}_w l_i}{w_i} \right) c_i^b. \quad (10)$$

With $\alpha_{i-1,i} = Z_i/(r_{i-1}^b + Z_i)$, $\gamma_i = e^{-\frac{\hat{r}_w l_i \sqrt{\hat{c}_w}}{2\sqrt{\hat{u}_w}}}$, and the effect of reflection, the voltage of the first overshoot, $V_{DD}^{'}$, at the receiving end after reflection equals $2\gamma_i Z_i V_{DD}/(r_{i-1}^b + Z_i)$, which may not equal V_{DD}. Thus, we can use an approximate method that divides t_c by $V_{DD}^{'}$ to obtain the charging time, $t_c^{'}$, for which the voltage equals $0.5V_{DD}$. Therefore, we have

$$\begin{aligned} t_c^{'} &= \ln 2 \left(Z_i + (1-\gamma_i)\frac{\hat{r}_w l_i}{w_i} \right) c_i^b / \left(\frac{2\gamma_i Z_i}{r_{i-1}^b + Z_i} \right) \\ &= \eta_i \left(r_{i-1}^b + \frac{\sqrt{\hat{u}_w}}{w_i \sqrt{\hat{c}_w}} \right) c_i^b, \end{aligned} \quad (11)$$

where

$$\begin{aligned} \eta_i &= \frac{\ln 2 \left(e^{\theta_i} + 2\theta_i \left(e^{\theta_i} - 1 \right) \right)}{2} \\ \theta_i &= \frac{\hat{r}_w l_i \sqrt{\hat{c}_w}}{2\sqrt{\hat{u}_w}}. \end{aligned}$$

Since transmission line analysis always gives the correct answer independent of the rise time of the driver, delay is the sum of the time-of-flight t_f along the wire and the time $t_c^{'}$ for charging the capacitive load [1], [19]. Thus, the propagation delay $\Delta(g_{i-1}, g_i)$ from the gate g_{i-1} to the next gate g_i in Figure 3 is given by

$$\Delta(g_{i-1}, g_i) = (2n-1)\frac{l_i}{v_i} + \eta_i \left(r_{i-1}^b + \frac{\sqrt{\hat{u}_w}}{w_i \sqrt{\hat{c}_w}} \right) c_i^b \quad (12)$$

where n is the number of required round trips to correctly transmit a signal.

F. Accuracy

We used SPICE to verify the accuracy of our delay model. The experiments were performed on a signal wire with no buffers. The parameters we used are listed in Table I, where $\hat{c}_w$, $\hat{u}_w$, $\hat{r}_w$, $\hat{c}_b$, $\hat{r}_b$, A_b, R_s, and C_L are the unit capacitance of a wire, the unit inductance of a wire, the sheet resistance of a wire, the unit capacitance and resistance of a gate, the area of minimum-size buffer, the driver resistance, and the load capacitance, respectively. This set of parameters is based on the 0.13 μm technology of the SIA'99 roadmap [23].

In the first and second experiments, we used fixed wire lengths (2.5 mm & 5 mm) with a variety of wire widths. The wire widths for all experiments satisfy Inequalities (5)–(7). Therefore, the wire widths ranged from 130 nm to 480 nm for the first experiment, and ranged from 130 nm to 530 nm for the second experiment. In Figure 5, the delays are plotted as functions of the wire widths for SPICE, Elmore, I&F, and our delay models, where I&F denotes the delay model presented in [11]. Tables II and III show the experimental results, where $Width$ denotes the wire width, $SPICE$ denotes the delay calculated by SPICE, $Elmore$ denotes the delay calculated by the Elmore delay model, E_Err denotes the percentage of the error between SPICE and the Elmore delay model, $I\&F$ denotes the delay calculated by the I&F delay model, $I\&F\_Err$ denotes the percentage of the error between SPICE and the I&F delay models, $Ours$ denotes the delay calculated by our delay model, and O_Err denotes the percentage of the error between SPICE and our delay models. The percentage of the error is calculated by $\frac{X-SPICE}{SPICE} \times 100\%$, where X denotes Elmore, I&F, or Ours. Compared to SPICE and

$\hat{c}_w$ $(fF/\mu m^2)$	$\hat{u}_w$ $(pH/\square)$	$\hat{r}_w$ $(\Omega/\square)$	$\hat{c}_b$ $(fF/\mu m)$	$\hat{r}_b$ $(k\Omega \cdot \mu m)$	A_b (μm^2)	R_s (Ω)	C_L (fF)
0.06	1.667	0.043	1.17	3.6	6.76	250	23.4

TABLE I
RC PARAMETERS OF THE 0.13 μm TECHNOLOGY IN SIA'99.

based on the lossy transmission line of 2.5 mm (5 mm) long, the maximum error calculated by the Elmore delay model is -36.13% (-19.58%) and the average error is 26.86% (12.05%), the maximum error calculated by the I&F delay model is -6.23% (11.34%) and the average error is 2.98% (4.70%), and the maximum error calculated by our delay model is 6.58% (12.38%) and the average error is 3.80% (6.22%).

In the third and fourth experiments, we used fixed wire widths (500 nm & 130 nm) with a variety of wire lengths. As mentioned earlier, the wire lengths for all experiments satisfy Inequalities (5)–(7). Therefore, the wire lengths ranged from 3.7 mm to 6.2 mm for the third experiment, and ranged from 0.82 mm to 7 mm for the fourth experiment. In Figure 6, the delays are plotted as functions of the wire lengths for SPICE, Elmore, I&F, and our delay models. Tables IV and V show the experimental results, where *Length* denotes the wire length. Compared to SPICE and based on the lossy transmission line of 500 nm (130 nm) wide, the maximum error calculated by the Elmore delay model is -10.01% (-51.74%) and the average error is 4.11% (30.55%), the maximum error calculated by the I&F delay model is 10.99% (-14.19%) and the average error is 9.52% (5.95%), and the maximum error calculated by our delay model is 1.99% (20.31%) and the average error is 1.49% (10.94%).

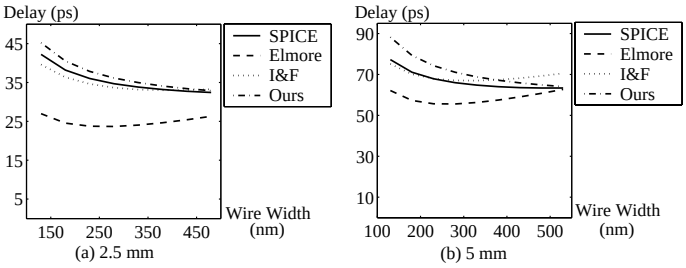

Fig. 5. Comparison of the delays calculated by SPICE, Elmore, I&F, and our delay models for lossy transmission lines; (a) wire length = 2.5 mm; (b) wire length = 5 mm.

According to the above four experiments, the average error of our delay model is 5.61%. Besides, based on the observation from the simulations, the delays computed from our model are upper bounds of those obtained by SPICE, which makes our model a reliable delay estimator under the lossy transmission line model. The Elmore delay model, however, has a significant negative percentage of errors. Therefore, the Elmore delay model is not a suitable delay estimator for the lossy transmission line model. Also, the I&F delay model incurs positive as well as negative errors

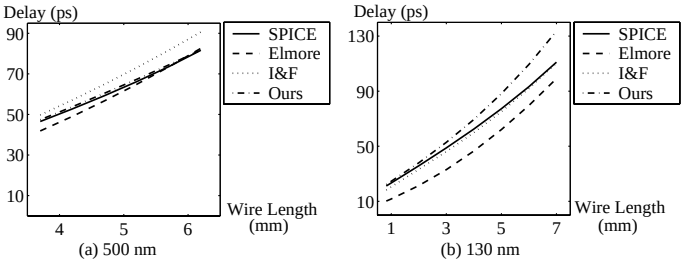

Fig. 6. Comparison of the delays calculated by SPICE, Elmore, I&F, and our delay models for lossy transmission lines; (a) wire width = 500 nm; (b) wire width = 130 nm.

for different wire widths of the same length. Hence, although the I&F delay model may be more accurate in some corner cases, it is less suitable for delay estimation under the lossy transmission line model when we apply wire sizing to optimize a circuit. Often circuit designers prefer overestimating delay to underestimate, since an over-optimistic estimation of delay may lead to timing violations. Therefore, our delay model should be more suitable than the Elmore and I&F delay models for practical applications. Notice that the maximum inaccuracy of our delay model occurs at the minimum wire size and the maximum wire length. The reason for this phenomenon is that the total resistance is comparable to the impedance. According to Section III-D, the transmission line behavior is insignificant for this situation.

IV. Problem Formulation

This paper targets at minimizing delay by sizing circuit components. We formulate this problem as follows:

- **Input:** A circuit path and the lower and upper bounds for wire and buffer sizes.
- **Objective:** Determine the optimal wire and buffer sizes for each segment in a circuit path, so that delay is minimized.

We will reformulate this problem for a routing tree in Section VI.

V. Optimal Wire and Buffer Sizing for a Path

A. Reflection Considerations

In practice, designers typically desire to optimize performance without generating undesirable reflections and transmit a signal correctly within a limited number of round trips. As the VLSI technology advances, the wire length is increasing and the capacitance of a gate is decreasing, making the time-of-flight delay dominate the de-

Width (nm)	SPICE (ps)	Elmore (ps)	E_Err (%)	I&F (ps)	I&F_Err (%)	Ours (ps)	O_Err (%)
130	42.23	26.97	-36.13	39.60	-6.23	45.20	6.58
180	38.20	24.55	-35.74	36.35	-4.85	40.51	5.69
230	36.02	23.74	-34.09	34.63	-3.86	37.85	4.84
280	34.69	23.69	-31.72	33.68	-2.92	36.15	4.03
330	33.81	24.04	-28.89	33.18	-1.86	34.96	3.28
380	33.19	24.65	-25.74	33.00	-0.58	34.08	2.61
430	32.74	25.41	-22.38	33.04	0.93	33.41	2.00
480	32.42	26.29	-18.90	33.27	2.61	32.88	1.39
Average			26.86		2.98		3.80

TABLE II

EXPERIMENTAL RESULTS FOR THE ACCURACY OF ELMORE, I&F, AND OUR DELAY MODELS FOR LOSSY TRANSMISSION LINES; WIRE LENGTH = 2.5 mm.

Width (nm)	SPICE (ps)	Elmore (ps)	E_Err (%)	I&F (ps)	I&F_Err (%)	Ours (ps)	O_Err (%)
130	77.28	62.15	-19.58	75.18	-2.72	88.20	12.38
180	71.12	57.30	-19.44	70.14	-1.38	79.32	10.34
230	67.89	55.68	-17.98	67.93	0.06	74.30	8.63
280	65.98	55.58	-15.77	67.07	1.65	71.08	7.17
330	64.78	56.29	-13.11	66.98	3.40	68.83	5.88
380	64.03	57.50	-10.20	67.40	5.27	67.17	4.68
430	63.59	59.03	-7.17	68.19	7.23	65.90	3.50
480	63.38	60.78	-4.10	69.26	9.28	64.89	2.33
530	63.37	62.70	-1.06	70.56	11.34	64.08	1.10
Average			12.05		4.70		6.22

TABLE III

EXPERIMENTAL RESULTS FOR THE ACCURACY OF ELMORE, I&F, AND OUR DELAY MODELS FOR LOSSY TRANSMISSION LINES; WIRE LENGTH = 5 mm.

Length (mm)	SPICE (ps)	Elmore (ps)	E_Err (%)	I&F (ps)	I&F_Err (%)	Ours (ps)	O_Err (%)
3.7	46.53	41.87	-10.01	49.75	6.92	47.39	1.84
4.2	52.77	49.04	-7.06	57.14	8.29	53.82	1.99
4.7	59.28	56.70	-4.35	64.91	9.49	60.46	1.98
5.2	66.16	64.85	-1.98	73.07	10.44	67.32	1.75
5.7	73.55	73.49	-0.08	81.63	10.99	74.42	1.19
6.2	81.65	82.62	1.19	90.63	10.99	81.80	0.18
Average			4.11		9.52		1.49

TABLE IV

EXPERIMENTAL RESULTS FOR THE ACCURACY OF SPICE, ELMORE, I&F, AND OUR DELAY MODELS FOR LOSSY TRANSMISSION LINES; WIRE WIDTH = 500 nm.

Length (mm)	SPICE (ps)	Elmore (ps)	E_Err (%)	I&F (ps)	I&F_Err (%)	Ours (ps)	O_Err (%)
0.82	21.18	10.22	-51.74	18.17	-14.19	22.30	5.31
1	23.37	11.75	-49.71	20.58	-11.96	24.58	5.16
2	35.81	21.41	-40.21	33.25	-7.16	37.97	6.03
3	48.81	33.03	-32.33	46.13	-5.50	52.84	8.26
4	62.56	46.61	-25.50	59.98	-4.13	69.47	11.05
5	77.28	62.15	-19.58	75.18	-2.72	88.20	14.13
6	93.30	79.65	-14.63	91.95	-1.45	109.41	17.27
7	111.02	99.11	-10.73	110.46	-0.50	133.57	20.31
Average			30.55		5.95		10.94

TABLE V

EXPERIMENTAL RESULTS FOR THE ACCURACY OF SPICE, ELMORE, I&F, AND OUR DELAY MODELS FOR LOSSY TRANSMISSION LINES; WIRE WIDTH = 130 nm.

lay. Therefore, we have the following theorem for the optimal number of round trips for delay optimization.

Theorem 1: Considering reflections, the minimum delay based on our model for a circuit section occurs when the

number of round trips equals one.

Proof: With the gate and the wire models described in Section III-A, we can divide a circuit path into sections, and the sections can be handled one by one. Consider a section shown in Figure 3. Suppose on the contrary that the minimum delay for a circuit section occurs when the number of round trips is larger than one. Let r_{i-1}^b and Z_i be the values that result in a (local) minimal delay for the circuit section when the number of round trips equals one, and r_{i-1}^{b*} and Z_i^* be the values that result in the globally minimum delay (the number of round trips is larger than one). According to Equation (12), we have the following:

$$D_1 = \frac{l_i}{v_i} + \eta_i \left(r_{i-1}^b + Z_i\right) c_i^b, \tag{13}$$

and

$$D_k = (2k-1)\frac{l_i}{v_i} + \eta_i \left(r_{i-1}^{b*} + Z_i^*\right) c_i^b, \tag{14}$$

where

$$\eta_i = \frac{\ln 2 \left(e^{\theta_i} + 2\theta_i \left(e^{\theta_i} - 1\right)\right)}{2}$$
$$\theta_i = \frac{\hat{r}_w l_i \sqrt{\hat{c}_w}}{2\sqrt{\hat{u}_w}},$$

D_1 is the (local) minimal delay when the number of round trips equals one, D_k is the globally minimum delay, and k is the number of round trips. Here, $k > 1$. Since $k > 1$ and a wire may need to be modeled as a transmission line if ringing occurs (see Section III-D), the first undershoot for D_k is smaller than V_{IH}, implying that the first undershoot for D_k is smaller that for D_1. The first undershoot can be calculated as follows:

$$V_u^1(x) = \frac{2x}{1+x}\gamma_i \left(1 + \frac{1-x}{1+x}\gamma_i^2\right), \tag{15}$$

where $x = x_i$ or x_i^*, $x_i = Z_i / r_{i-1}^b$, and $x_i^* = Z_i^* / r_{i-1}^{b*}$. On one hand, if $V_u^1(x)$ increases as x increases, $x_i > x_i^*$, implying that $r_{i-1}^{b*} Z_i > r_{i-1}^b Z_i^*$. On the other hand, if $V_u^1(x)$ decreases as x increases, $x_i < x_i^*$, implying that $r_{i-1}^{b*} Z_i < r_{i-1}^b Z_i^*$. To show that $D_k > D_1$, we need to discuss the following two cases:

Case 1. $r_{i-1}^{b*} Z_i > r_{i-1}^b Z_i^*$:

Case 1.1 $r_{i-1}^{b*} > r_{i-1}^b$ and $Z_i^* = Z_i$:

The first and second terms of Equation (14) are always larger than those of Equation (13). Thus, $D_k > D_1$.

Case 1.2 $Z_i^* < Z_i$ and $r_{i-1}^{b*} = r_{i-1}^b$:

Subtracting Equation (14) from Equation (13), we have

$$D_k - D_1 = (2k-2)\frac{l_i}{v_i} + \eta_i \left(Z_i^* - Z_i\right) c_i^b. \tag{16}$$

By Equation (7), we have

$$x < \frac{1-\gamma_i^2}{4\gamma_i - \gamma_i^2 - 1}. \tag{17}$$

When $\gamma_i = 1/e$ (≈ 0.37), x can be as larger as $\frac{e^2-1}{4e-1-e^2}$ (≈ 2.57). By Inequalities (8) and (17), we have the range of x as follows:

$$1 < x < \frac{e^2-1}{4e-1-e^2}. \tag{18}$$

Therefore, by Inequality (18), Inequality (16) can be rewritten as follows:

$$\begin{aligned} D_k - D_1 &> (2k-2)\frac{l_i}{v_i} + \eta_i \left(r_{i-1}^{b*} - \frac{e^2-1}{4e-1-e^2} r_{i-1}^b\right) c_i^b \\ &> (2k-2)\frac{l_i}{v_i} + \eta_i \left(r_{i-1}^b - 3r_{i-1}^b\right) c_i^b \\ &> (2k-2)\frac{l_i}{v_i} - 2\eta_i r_{i-1}^b (c_i^b + \hat{c}_w w_i l_i) \\ &> (2k-2)\frac{l_i}{v_i} - \frac{2}{1.1}\eta_i \frac{l_i}{v_i}. \end{aligned} \tag{19}$$

According to Inequality (6), the minimum of the right-hand side of Inequality (19) occurs when $\theta_i = 1$, resulting in the minimum value $0.12\ l_i/v_i$. Thus, we have $D_k > D_1$.

Case 1.3 $r_{i-1}^{b*} > r_{i-1}^b$ and $Z_i^* < Z_i$:

According to Case 1.1 and Case 1.2, $D_k > D_1$.

Case 1.4 $r_{i-1}^{b*} < r_{i-1}^b$ and $Z_i^* < Z_i$:

Let $r_{i-1}^b = y_1 r_{i-1}^{b*}$ and $Z_i = y_2 Z_i^*$, where y_1, $y_2 > 1$. Since $r_{i-1}^{b*} Z_i > r_{i-1}^b Z_i^*$, $y_1 < y_2$. The first undershoot caused by $r_{i-1}^{b'}$ and $Z_i^{'}$ is the same as that caused by r_{i-1}^b and Z_i, where $r_{i-1}^{b'} = r_{i-1}^b / y_1$ and $Z_i^{'} = Z_i / y_1$. Substituting $r_{i-1}^{b'}$ for r_{i-1}^b and $Z_i^{'}$ for Z_i, the second term of Equation (13) becomes smaller. Therefore, when the number of round trips equals one, $r_{i-1}^{b'}$ and $Z_i^{'}$ lead to a (local) minimal delay for the circuit section, contradicting the assumption that r_{i-1}^b and Z_i give a (local) minimal delay for the circuit section. Thus, the case that $r_{i-1}^{b*} < r_{i-1}^b$ and $Z_i^* < Z_i$ will never happen.

Case 1.5 $r_{i-1}^{b*} > r_{i-1}^b$ and $Z_i^* > Z_i$:

Let $r_{i-1}^{b*} = y_3 r_{i-1}^b$ and $Z_i^* = y_4 Z_i$, where y_3, $y_4 > 1$. Since $r_{i-1}^{b*} Z_i > r_{i-1}^b Z_i^*$, $y_3 > y_4$. Similar to Case 1.4, $r_{i-1}^{b*'}$ and $Z_i^{*'}$ lead to the globally minimum delay, where $r_{i-1}^{b*'} = r_{i-1}^{b*} / y_4$ and $Z_i^{*'} = Z_i^* / y_4$, contradicting the assumption that $r_{i-1}^{b*'}$ and $Z_i^{*'}$ give the globally minimum delay. Thus, the case that $r_{i-1}^{b*} > r_{i-1}^b$ and $Z_i^* > Z_i$ will never happen.

Case 2. $r_{i-1}^{b*} Z_i < r_{i-1}^b Z_i^*$:

Case 2.1 $r_{i-1}^{b*} < r_{i-1}^b$ and $Z_i^* = Z_i$:

Subtracting Equation (14) from Equation (13), we have

$$\begin{aligned} D_k - D_1 &= (2k-2)\frac{l_i}{v_i} + \eta_i \left(r_{i-1}^{b*} - r_{i-1}^b\right) c_i^b \\ &> (2k-2)\frac{l_i}{v_i} - \eta_i r_{i-1}^b c_i^b \\ &> (2k-2)\frac{l_i}{v_i} - \eta_i r_{i-1}^b (\hat{c}_w w_i l_i + c_i^b) \\ &> (2k-2)\frac{l_i}{v_i} - \frac{1}{1.1}\eta_i \frac{l_i}{v_i}. \end{aligned} \tag{20}$$

According to Inequality (6), the minimum of the right-hand

side of Inequality (20) occurs when $\theta_i = 1$, resulting in the minimum value 2.06 l_i/v_i. Thus, we have $D_k > D_1$.
Case 2.2 $Z_i^* > Z_i$ and $r_{i-1}^{b*} = r_{i-1}^b$:
The first and second terms of Equation (14) are always larger than those of Equation (13). Thus, $D_k > D_1$.
Case 2.3 $r_{i-1}^{b*} < r_{i-1}^b$ and $Z_i^* > Z_i$:
According to Case 2.1 and Case 2.2, $D_k > D_1$.
Case 2.4. $r_{i-1}^{b*} < r_{i-1}^b$ and $Z_i^* < Z_i$:
Let $r_{i-1}^b = y_5 r_{i-1}^{b*}$ and $Z_i = y_6 Z_i^*$, where y_5, $y_6 > 1$. Since $r_{i-1}^{b*} Z_i < r_{i-1}^b Z_i^*$, $y_5 > y_6$. Similar to Case 1.4, $r_{i-1}^{b'}$ and $Z_i^{'}$ lead to a (local) minimum delay, where $r_{i-1}^{b'} = r_{i-1}^b/y_6$ and $Z_i^{'} = Z_i/y_6$, contradicting the assumption that r_{i-1}^b and Z_i give a (local) minimal delay for the circuit section. Thus, the case that $r_{i-1}^{b*} < r_{i-1}^b$ and $Z_i^* < Z_i$ will never happen.
Case 2.5. $r_{i-1}^{b*} > r_{i-1}^b$ and $Z_i^* > Z_i$:
Let $r_{i-1}^{b*} = y_7 r_{i-1}^b$ and $Z_i^* = y_8 Z_i$, where y_7, $y_8 > 1$. Since $r_{i-1}^b Z_i < r_{i-1}^b Z_i^*$, $y_7 < y_8$. Similar to Case 1.4, $r_{i-1}^{b*'}$ and $Z_i^{*'}$ lead to the globally minimum delay, where $r_{i-1}^{b*'} = r_{i-1}^{b*}/y_7$ and $Z_i^{*'} = Z_i^*/y_7$, contradicting the assumption that $r_{i-1}^{b*'}$ and $Z_i^{*'}$ give the globally minimum delay. Thus, the case that $r_{i-1}^{b*} > r_{i-1}^b$ and $Z_i^* > Z_i$ will never happen.

Therefore, the globally minimum delay occurs when the number of round trips equals one. ■

According to Theorem 1, we can rewrite Equation (12) as follows:

$$\Delta(g_{i-1}, g_i) = l_i\sqrt{\hat{u}_w \hat{c}_w} + \eta_i \left(r_{i-1}^b + \frac{\sqrt{\hat{u}_w}}{w_i \sqrt{\hat{c}_w}} \right) c_i^b, \quad (21)$$

where

$$\eta_i = \frac{\ln 2 \left(e^{\theta_i} + 2\theta_i \left(e^{\theta_i} - 1 \right) \right)}{2}$$
$$\theta_i = \frac{\hat{r}_w l_i \sqrt{\hat{c}_w}}{2\sqrt{\hat{u}_w}}.$$

B. Optimal Wire Sizing

In this section, we minimize the delay of a circuit path by wire sizing. If all buffer sizes and locations are fixed, the delay function of a circuit path from the source s to sink t with $n+1$ segments (w_1, ..., w_{n+1}) can be calculated as follows:

$$\begin{aligned}\Delta(s,t) &= \sum_{i=1}^{n+1} l_i\sqrt{\hat{u}_w \hat{c}_w} + \eta_1 \left(R_S + \frac{\sqrt{\hat{u}_w}}{w_1 \sqrt{\hat{c}_w}} \right) c_1^b \\ &+ \sum_{i=2}^{n} \eta_i \left(r_{i-1}^b + \frac{\sqrt{\hat{u}_w}}{w_i \sqrt{\hat{c}_w}} \right) c_i^b \\ &+ \eta_{n+1} \left(r_n^b + \frac{\sqrt{\hat{u}_w}}{w_{n+1} \sqrt{\hat{c}_w}} \right) C_L, \quad (22)\end{aligned}$$

where

$$\eta_i = \frac{\ln 2 \left(e^{\theta_i} + 2\theta_i \left(e^{\theta_i} - 1 \right) \right)}{2}$$
$$\theta_i = \frac{\hat{r}_w l_i \sqrt{\hat{c}_w}}{2\sqrt{\hat{u}_w}}.$$

Notice that Equation (22) is a posynomial function in w_1, ..., w_{n+1}, implying that the wire-sizing problem has a unique global minimum [2], [7]. Thus, we can apply any efficient search algorithm, such as the well-known gradient search procedure, to find a locally optimal solution and thus the globally optimal solution.

Theorem 2: With fixed buffer sizes and locations, the delay of a circuit path based on our model is a posynomial function in wire sizes.

C. Optimal Buffer Sizing

In this section, we minimize the delay of a circuit path by buffer sizing. If all wire sizes and buffer locations are fixed, the delay function of a circuit path from the source s to sink t with n segments (g_1, ..., g_n) can be calculated as follows:

$$\begin{aligned}\Delta(s,t) &= \sum_{i=1}^{n+1} l_i\sqrt{\hat{u}_w \hat{c}_w} + \eta_1 \left(R_S + \frac{\sqrt{\hat{u}_w}}{w_1 \sqrt{\hat{c}_w}} \right) \hat{c}_b g_1 \\ &+ \sum_{i=2}^{n} \eta_i \left(\frac{\hat{r}_b}{g_{i-1}} + \frac{\sqrt{\hat{u}_w}}{w_i \sqrt{\hat{c}_w}} \right) \hat{c}_b g_i \\ &+ \eta_{n+1} \left(\frac{\hat{r}_b}{g_n} + \frac{\sqrt{\hat{u}_w}}{w_{n+1} \sqrt{\hat{c}_w}} \right) C_L, \quad (23)\end{aligned}$$

where

$$\eta_i = \frac{\ln 2 \left(e^{\theta_i} + 2\theta_i \left(e^{\theta_i} - 1 \right) \right)}{2}$$
$$\theta_i = \frac{\hat{r}_w l_i \sqrt{\hat{c}_w}}{2\sqrt{\hat{u}_w}}.$$

Notice that Equation (23) is also a posynomial function in g_1, ..., g_n, implying that the buffer-sizing problem has a unique global minimum [2], [7]. Thus, we can apply any efficient search algorithm, such as the well-known gradient search procedure, to find a locally optimal solution and thus the globally optimal solution.

Theorem 3: With fixed wire sizes and buffer locations, the delay of a circuit path based on our model is a posynomial function in buffer sizes.

D. Optimal Simultaneous Wire and Buffer Sizing

In this section, we minimize the delay of a circuit path by simultaneous wire and buffer sizing. If all buffer locations are fixed, the delay function of a circuit path from the source s to sink t with $2n+1$ segments (w_1, ..., w_{n+1}, g_1, ..., g_n) is the same as Equation (23).

Notice that Equation (23) is also a posynomial function in w_1, ..., w_{n+1}, g_1, ..., g_n, implying that the simultaneous wire- and buffer-sizing problem has a unique global minimum [2], [7]. Thus, we can apply any efficient search algorithm, such as the well-known gradient search procedure, to find a locally optimal solution and thus the globally optimal solution.

Theorem 4: With fixed buffer locations, the delay of a circuit path based on our model is a posynomial function in wire and buffer sizes.

VI. Extensions to Wire and Buffer Sizing for a Routing Tree

Given a routing tree, our objective is to minimize the critical path delay under the constraints that the first undershoot at each branching point is within the same signal level, and the number of round trips required for correctly transmitting a signal from the root to each load is at most one. We formulate this problem as follows:

- **Input:** A routing tree and the lower and upper bounds for wire and buffer sizes.
- **Output:** Determine the optimal wire and buffer sizes of the tree, so that the critical path delay is minimized under the constraints that the first undershoot is within the same signal level, and the number of round trips is at most one.

We shall first discuss the problem on binary routing trees, and then apply the technique to general routing trees.

A. Reflection Constraints

As shown in Figure 7, when a signal is sent out from the source R_S and passes through the point 1 to the point 2, a reflection may be generated at the point 2 and travels backward to the point 1. When the reflection reaches the point 1, the voltage at the point 1 will be interfered. Further, if a reflection propagated down to one load is large enough, it could cause logic failure at the load. To prevent

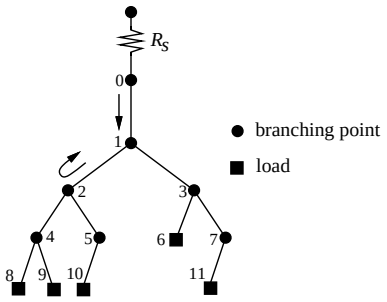

Fig. 7. A signal is sent out from the point 0 and then passes through the point 1 to the point 2.

from falsely triggering the load, the reflection coefficient at each node must be large enough. For the example shown in Figure 7, if the reflection coefficient $\beta_{1,0}$ at the point 1 is larger, the reflections generated at the points 2 and 3 have smaller impact on the point 1. According to [1], the reflection coefficient $\beta_{1,0}$ is given by

$$\beta_{1,0} = \frac{Z_2Z_3 - Z_1Z_2 - Z_1Z_3}{Z_1Z_2 + Z_1Z_3 + Z_2Z_3}. \tag{24}$$

By Equation (24), $\beta_{1,0}$ becomes larger when Z_1Z_2 and Z_1Z_3 are smaller. If $\beta_{1,0}$ becomes larger, the transmission coefficient $\alpha_{2,1} = \frac{2Z_1Z_3}{Z_1Z_2+Z_1Z_3+Z_2Z_3}$ is smaller. When a reflection generated at the point 2 travels backward to the point 1, the impact of the reflection may be negligible if $\alpha_{2,1}$ is small enough. Similarly, the impact of the reflections generated at the point 3 on other points can also be negligible. For each point i of a routing tree, if the reflections generated at the point i have little interference at other points, a signal can be correctly transmitted from the source to the loads. In order to correctly transmit a signal from the source of a routing tree to each load, the voltage at each branching point must be larger than or equal to the threshold voltage V_{IH} within one round trip. As shown in Figure 8, the following constraint must be satisfied for the point i:

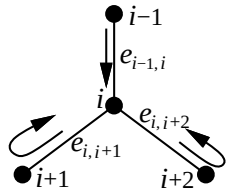

Fig. 8. A signal is sent from the point $i-1$ to the point i, and then $i+1$ and $i+2$. The impact of the reflections generated at the points $i+1$ and $i+2$ on the point i may be negligible if $\alpha_{i+1,i}$ and $\alpha_{i+2,i}$ are small enough.

$$\alpha_{i-1,i}\gamma_{e_{i-1,i}}(1+\beta_{i,i-1}) \geq V_{IH}. \tag{25}$$

Based on Inequality (25), the initial voltage at the point i will be greater than or equal to the threshold voltage when a signal from the point $i-1$ arrives at the point i. Let $e_{i,j}$ denote the edge between the points i and j, and $\tau_{i,j}$ represent the length of $e_{i,j}$. Since $\tau_{i-1,i}$, $\tau_{i,i+1}$, and $\tau_{i,i+2}$ in Figure 8 could be different, the reflections generated at those points will arrive at the point i at different times. Without loss of generality, assume that $\tau_{i,i+1} \leq \tau_{i,i+2} \leq \tau_{i-1,i}$. The first reflection arrives at the point i is sent out from the point $i+1$, next is from the point $i+2$, and the last is generated from the point $i-1$. In order to prevent the reflections from changing the signal level at the point i, we have the following constraints:

$$\alpha_{i-1,i}\gamma_{e_{i-1,i}}(1+\beta_{i,i-1}+\alpha_{i,i+1}\gamma^2_{e_{i,i+1}}\beta_{i+1,i}\alpha_{i,i-1}) \geq V_{IH} \tag{26}$$

$$\text{left-hand side of (26)} + \alpha_{i-1,i}\gamma_{e_{i-1,i}}\alpha_{i,i+2}\gamma^2_{e_{i,i+2}}\beta_{i+2,i}\alpha_{i,i-1} \geq V_{IH} \tag{27}$$

$$\text{left-hand side of (27)} + \alpha_{i-1,i}\gamma^3_{e_{i-1,i}}\beta_{i,i-1}\beta_{i-1,i}(1+\beta_{i,i-1}) \geq V_{IH}. \tag{28}$$

If all constraints are satisfied, the reflection coefficient at each point will be large enough, implying that the reflections generated at the point i have little interference at other points. As a result, a signal can be correctly transmitted from the source to the loads in a tree.

B. Delay Calculation

Given a routing tree, we number its nodes level by level, and from left to right on each level (see Figure 7). Let m, L, and P denote the number of edges in the tree, the set of loads, and the critical path, respectively. Similar to Equtaion (12), the critical path delay of a routing tree from the source s to a load t is given by

$$\begin{aligned}\Delta(s,t) &= \sum_{e_{i,j}\in P}(2n_{i,j}-1)\frac{\tau_{i,j}}{v_{i,j}} \\ &+ \sum_{e_{i,j}\in P, j\in L}\xi_{i,j}(R_s+Z_{i,j})c_j,\end{aligned} \tag{29}$$

where

$$\xi_{i,j} = \frac{\ln 2\left(e^{\vartheta_{i,j}}+2\vartheta_{i,j}\left(e^{\vartheta_{i,j}}-1\right)\right)}{2}$$

$$\vartheta_{i,j} = \frac{\hat{r}_w \tau_{i,j} \sqrt{\hat{c}_w}}{2\sqrt{\hat{u}_w}},$$

c_i denotes the capacitance of node i, $v_{i,j}$ and $Z_{i,j}$ denote the propagation velocity and the impedance of edge $e_{i,j}$, respectively.

We used SPICE to verify the accuracy of our delay model. The experiments were performed on a binary routing tree with no buffers (as shown in Figure 9). Table VI shows the parameters and the experimental results, where R_S denotes the driver resistance, *Length* and *Width* denote the length and width of each segment, *Load* denotes the load capacitance of segments 2 and 3, *SPICE* denotes the delay calculated by SPICE, *Elmore* denotes the delay calculated by the Elmore delay model, *E_Err* denotes the percentage of the error between SPICE and the Elmore delay model, *Ours* denotes the delay calculated by our delay model, and *O_Err* denotes the percentage of the error between SPICE and our delay model. The percentage of the error is calculated by $\frac{X-SPICE}{SPICE} \times 100\%$, where X denotes Elmore or Ours.

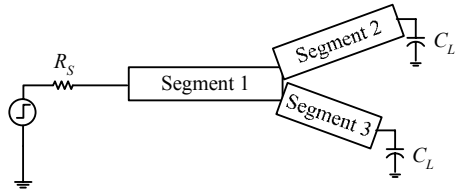

Fig. 9. A binary routing tree without buffers.

We propose Algorithm *Find-Critical-Path* (summarized in Figure 10) to find the critical path of a routing tree T. First, we determine the number of round trips $n_{i,j}$ along edge $e_{i,j}$ required to correctly transmit a signal (Line 2). The number of round trips is the minimum $n_{i,j}$ that satisfies the following constraint:

$$\sum_{t=1}^{n_{i,j}} \alpha_{i,j} \gamma_{e_{i,j}}^{2t-1} \beta_{i,j}^{t-1} \beta_{j,i}^{t} \geq V_{IH}.$$

After determining the number of round trips on each edge, we label each edge with the weight $n_{i,j}\tau_{i,j}$ (Line 3). The critical path delay is the sum of edge weights along the longest path. We then apply the depth first traversal to compute the longest path in $O(p)$ time, where p is the number of nodes (Line 4).

C. General Routing Tree

We extend the technique discussed in previous subsections to general routing trees. As shown in Figure 11, assume that the point i has k children, and a signal is sent out from the point $i-1$ and then propagates down to the children of the point i. Without loss of generality, assume that $\tau_{i,i+1} \leq \tau_{i,i+2} \leq \cdots \leq \tau_{i,i+k} \leq \tau_{i-1,i}$. To prevent the reflections generated at the children from changing the signal level at the point i, we have the following constraints:

Algorithm: *Find-Critical-Path*(T)
Input: T–a routing tree
Output: the critical path
begin
1 **for** each edge $e_{i,j}$ in T
2 Determine the number of round trips $n_{i,j}$ on $e_{i,j}$.
3 Label $e_{i,j}$ with the weight $n_{i,j}\tau_{i,j}$.
4 Call a depth-first traversal to find the longest path.
5 **return** the longest path
end

Fig. 10. The Algorithm for determining the critical path of a tree.

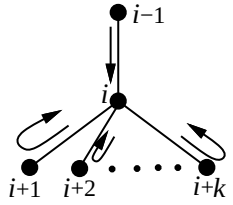

Fig. 11. The point i has k children, and the signal is sent from the point $i-1$ to other points.

$$\begin{array}{rl} & \alpha_{i-1,i}\gamma_{e_{i-1,i}}(1+\beta_{i,i-1}+\alpha_{i,i+1}\gamma_{e_{i,i+1}}^2\beta_{i+1,i}\alpha_{i,i-1} \geq V_{IH} \\ \text{left-hand side of the preceding row} & +\alpha_{i-1,i}\gamma_{e_{i-1,i}}\alpha_{i,i+2}\gamma_{e_{i,i+2}}^2\beta_{i+2,i}\alpha_{i,i-1} \geq V_{IH} \\ & \vdots \\ \text{left-hand side of the preceding row} & +\alpha_{i-1,i}\gamma_{e_{i-1,i}}\alpha_{i,i+k}\gamma_{e_{i,i+k}}^2\beta_{i+k,i}\alpha_{i,i-1} \geq V_{IH} \\ \text{left-hand side of the preceding row} & +\alpha_{i-1,i}\gamma_{e_{i-1,i}}^3\beta_{i,i-1}\beta_{i-1,i}(1+\beta_{i,i-1}) \geq V_{IH}. \end{array}$$

If all constraints are satisfied, the reflection coefficient at each point will be large enough; thus, a signal can be correctly transmitted from the source to the loads in a general routing tree.

D. Our Algorithm

Our objective is to minimize the critical path delay of a routing tree under the constraints that a signal can be correctly transmitted within one round trip and the reflection is sufficiently small to prevent from falsely triggering loads. Since the delay of a tree is dominated by the critical path delay, our problem is to find the wire sizes $\vec{w} = (w_1, w_2, \cdots, w_n)$ that minimize the critical path delay $\Delta(s,t)$ of a tree subject to the constraints listed in Inequalities (25)–(28). We can apply any search algorithm such as the well-known gradient search procedure to find a solution. Algorithm *Minimize-Tree-Delay* computes the minimum delay of a routing tree (see Figure 12). It consists of two stages. The first stage applies the procedure *Find-Critical-Path* to compute the critical path of a routing tree. The second stage applies the gradient search procedure to determine the wire sizes that minimize the critical path delay. We repeat the two stages until no improvements on the delay of the tree.

Experimental ID	Segment ID	Parameter				Experimental Result				
		R_S (Ω)	Length (mm)	Width (μm)	Load (fF)	SPICE (ps)	Elmore (ps)	E_Err (%)	Ours (ps)	O_Err (%)
1	1	10	1	1	–	–	–	–	–	–
	2	–	1	1	23.4	22.80	13.03	-42.87	21.68	-4.91
	3	–	1	1	23.4	22.80	13.03	-42.87	21.68	-4.91
2	1	10	1	1	–	–	–	–	–	–
	2	–	0.9	1	23.4	21.80	11.41	-47.67	20.65	-5.27
	3	–	0.7	1	23.4	19.70	10.79	-45.20	18.59	-5.62
3	1	10	1	1	–	–	–	–	–	–
	2	–	0.9	1.2	23.4	21.30	11.39	-46.55	20.39	-4.27
	3	–	0.7	0.8	23.4	20.40	11.10	-45.60	18.97	-7.02
4	1	10	1.5	1	–	–	–	–	–	–
	2	–	1.3	1.2	23.4	30.80	21.11	-31.47	29.50	-4.21
	3	–	1	0.8	23.4	29.00	20.39	-29.70	27.08	-6.63
5	1	10	2	1	–	–	–	–	–	–
	2	–	1.7	1.2	23.4	41.10	33.75	-17.89	38.63	-6.00
	3	–	1.3	0.8	23.4	36.70	32.41	-11.69	35.20	-4.08
Average								36.15		5.29

TABLE VI

PARAMETERS AND EXPERIMENTAL RESULTS FOR THE ACCURACY OF ELMORE AND OUR DELAY MODELS ON A BINARY ROUTING TREE WITH NO BUFFERS.

Algorithm: *Minimize-Tree-Delay*(T)
Input: T–a routing tree.
Output: wire sizes $\vec{w} = (w_1, w_2, \cdots, w_n)$
begin
1 **repeat**
2 *critical-path* $\leftarrow$ *Find-Critical-Path*(T)
3 $w \leftarrow$ *Gradient-Search-Procedure*(*critical-path*)
4 **until** no improvement on the delay of T
end

Fig. 12. The Alogrithm for minimizing the delay of a tree.

E. Simultaneous Wire and Buffer Sizing for a Routing Tree

Based on the gate and wire models presented in Section III, we can divide a buffered routing tree into subtrees. In Figure 13, the routing tree is divided into three subtrees. We can treat each subtree as a routing tree with no buffers, and then obtain the reflection constraints for each subtree. Thus, we can minimize the delay of a buffered routing tree under the constraints that a signal can be correctly transmitted within one round trip, and the first undershoot is controlled to prevent from changing the signal level if the reflection constraints for each subtree are satisfied.

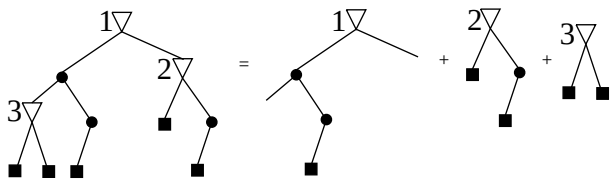

Fig. 13. A routing tree with buffers.

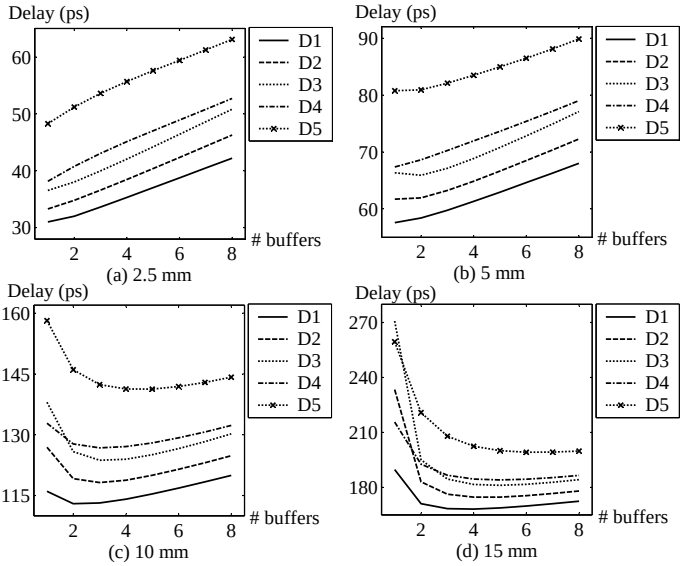

Fig. 14. Comparison of different optimization techniques; D1: simultaneous wire and buffer sizing; D2 & D3: wire sizing alone, and the gate resistances are 90 Ω and 60 Ω, respectively; D4 & D5: buffer sizing alone, and the wire widths are 0.3 μm and 0.13 μm, respectively.

VII. EXPERIMENTAL RESULTS

We used the nonlinear programming solver, the LINGO 6.0 system, on an Intel Pentium II 400 MHz PC to compute the optimal wire and buffer sizes in a circuit path. All computations are less than 1 *sec*. The parameters used are listed in Table I.

Given four lines of the lengths 2.5 mm, 5 mm, 10 mm, and 15 mm, we inserted a specified number of buffers at equidistance. Then, we applied wire and/or buffer sizing to minimize delay. Listed in Tables VII, VIII, IX, and X, Column D1 gives the delays and areas by sizing wires and

# buffers	D1		D2		D3		D4		D5	
	Delay (ps)	Area ($K\mu m^2$)	Delay (ps)	Area ($K\mu m^2$)	Delay (ps)	Area ($K\mu m^2$)	Delay (ps)	Area ($K\mu m^2$)	Delay (ps)	Area ($K\mu m^2$)
1	31.00	4.48	33.30	8.52	36.54	8.66	38.15	0.81	48.29	0.37
2	32.00	7.76	34.81	10.31	38.04	10.58	40.77	0.84	51.20	0.39
3	33.63	8.36	36.59	11.31	39.97	11.71	43.06	0.86	53.60	0.39
4	35.32	8.76	38.47	12.00	42.06	12.54	45.12	0.87	55.69	0.40
5	37.03	9.05	40.40	12.54	44.21	13.22	47.03	0.87	57.60	0.40
6	38.75	9.29	42.34	13.01	46.40	13.82	48.91	0.89	59.41	0.40
7	40.48	9.50	44.31	13.42	48.61	14.37	50.80	0.90	61.24	0.41
8	42.21	9.69	46.28	13.80	50.83	14.89	52.71	0.92	63.10	0.42

TABLE VII

EXPERIMENTAL RESULTS; D1: SIMULTANEOUS WIRE AND BUFFER SIZING; D2 & D3: WIRE SIZING ALONE, AND THE GATE RESISTANCES ARE 90 Ω AND 60 Ω, RESPECTIVELY; D4 & D5: BUFFER SIZING ALONE, AND THE WIRE WIDTHS ARE 0.3 μm AND 0.13 μm, RESPECTIVELY; PATH LENGTH $= 2.5\ mm$.

# buffers	D1		D2		D3		D4		D5	
	Delay (ps)	Area ($K\mu m^2$)	Delay (ps)	Area ($K\mu m^2$)	Delay (ps)	Area ($K\mu m^2$)	Delay (ps)	Area ($K\mu m^2$)	Delay (ps)	Area ($K\mu m^2$)
1	57.57	11.98	61.69	15.94	66.33	16.07	67.37	1.56	80.76	0.70
2	58.39	14.64	61.92	19.68	65.90	19.95	68.62	1.59	80.93	0.71
3	59.76	15.95	63.23	21.56	67.13	21.97	70.27	1.61	82.09	0.72
4	61.31	16.75	64.86	22.76	68.85	23.30	71.96	1.62	83.49	0.72
5	62.94	17.30	66.64	23.62	70.79	24.30	73.63	1.63	84.96	0.73
6	64.61	17.73	68.48	24.31	72.83	25.12	75.38	1.64	86.49	0.73
7	66.29	18.07	70.37	24.89	74.93	25.84	77.18	1.66	88.13	0.74
8	68.00	18.34	72.29	25.39	77.09	26.48	79.02	1.67	89.85	0.74

TABLE VIII

EXPERIMENTAL RESULTS; D1: SIMULTANEOUS WIRE AND BUFFER SIZING; D2 & D3: WIRE SIZING ALONE, AND THE GATE RESISTANCES ARE 90 Ω AND 60 Ω, RESPECTIVELY; D4 & D5: BUFFER SIZING ALONE, AND THE WIRE WIDTHS ARE 0.3 μm AND 0.13 μm, RESPECTIVELY; PATH LENGTH $= 5\ mm$.

# buffers	D1		D2		D3		D4		D5	
	Delay (ps)	Area ($K\mu m^2$)	Delay (ps)	Area ($K\mu m^2$)	Delay (ps)	Area ($K\mu m^2$)	Delay (ps)	Area ($K\mu m^2$)	Delay (ps)	Area ($K\mu m^2$)
1	116.01	19.33	126.88	28.94	138.03	29.07	132.84	3.06	158.16	1.35
2	112.97	26.38	119.17	37.43	125.81	37.70	127.72	3.09	146.04	1.36
3	113.14	29.77	118.20	41.48	123.71	41.88	126.76	3.11	142.37	1.37
4	114.10	31.76	118.78	43.88	123.93	44.42	127.07	3.12	141.28	1.37
5	115.39	33.01	119.98	45.49	125.05	46.17	127.97	3.14	141.27	1.38
6	116.83	33.93	121.45	46.70	126.57	47.51	129.23	3.15	141.90	1.38
7	118.36	34.63	123.08	47.65	128.31	48.59	130.69	3.17	142.92	1.39
8	119.94	35.19	124.81	48.43	130.20	49.52	132.28	3.18	144.19	1.40

TABLE IX

EXPERIMENTAL RESULTS; D1: SIMULTANEOUS WIRE AND BUFFER SIZING; D2 & D3: WIRE SIZING ALONE, AND THE GATE RESISTANCES ARE 90 Ω AND 60 Ω, RESPECTIVELY; D4 & D5: BUFFER SIZING ALONE, AND THE WIRE WIDTHS ARE 0.3 μm AND 0.13 μm, RESPECTIVELY; PATH LENGTH $= 10\ mm$.

buffers simultaneously (denoted by SWBS); Column D2 (D3) gives the delays and areas by sizing wires alone (denoted by WS), with the resistance of each gate equal to 90 Ω (60 Ω); and Column D4 (D5) lists the delays and areas by sizing buffers alone (denoted by BS) with the fixed wire width of 0.3 μm (0.13 μm), where the area is the sum of wire area (the product of width and length) and buffer area (the product of buffer size and the area of minimum-size buffer). In Figures 14(a), (b), (c), and (d), the path delays are plotted as functions of the number of buffers for the five optimization techniques D1, D2, D3, D4, and D5.

As shown in Figure **??**, the ranking of those techniques for optimizing circuit performance, from the most effective to the least, is given by SWBS $\succ$ WS $\succ$ BS. These phenomena show the effectiveness of simultaneous wire and buffer sizing under the transmission line model. Further, the number of buffers required for performance optimization is quite small for simultaneous wire and buffer sizing. Since the delay is inversely proportional to the voltage at the receiving end, and voltage attenuation increases as wire

# buffers	D1		D2		D3		D4		D5	
	Delay (ps)	Area ($K\mu m^2$)	Delay (ps)	Area ($K\mu m^2$)	Delay (ps)	Area ($K\mu m^2$)	Delay (ps)	Area ($K\mu m^2$)	Delay (ps)	Area ($K\mu m^2$)
1	189.68	19.98	233.42	39.94	270.83	40.07	215.65	4.60	259.48	2.00
2	171.05	35.27	183.03	54.21	195.01	54.48	192.62	4.59	220.81	2.01
3	168.41	41.63	176.29	60.73	184.54	61.13	186.61	4.61	207.95	2.02
4	168.17	45.28	174.66	64.52	181.60	65.06	184.54	4.63	202.47	2.02
5	168.79	47.61	174.70	67.02	181.10	67.69	184.09	4.65	200.05	2.03
6	169.81	49.23	175.48	68.81	181.66	69.63	184.49	4.66	199.21	2.04
7	171.05	50.45	176.65	70.19	182.77	71.14	185.35	4.68	199.24	2.05
8	172.43	51.39	178.04	71.30	184.20	72.38	186.50	4.69	199.79	2.05

TABLE X

EXPERIMENTAL RESULTS; D1: SIMULTANEOUS WIRE AND BUFFER SIZING; D2 & D3: WIRE SIZING ALONE, AND THE GATE RESISTANCES ARE 90 Ω AND 60 Ω, RESPECTIVELY; D4 & D5: BUFFER SIZING ALONE, AND THE WIRE WIDTHS ARE 0.3 μm AND 0.13 μm, RESPECTIVELY; PATH LENGTH = 15 mm.

length increases, inserting buffers can partition a wire into sections of smaller length, which decreases the voltage attenuation and also the path delay.

VIII. Conclusions

In this paper, we have presented an analytical model for computing the delay of a wire under the transmission line model. Extensive simulations have shown the high fidelity of our model. Compared with previous works [8], [11], our model leads to smaller average errors in delay estimation. Based on our model, we have shown the property that the minimum delay for a transmission line with reflection occurs when the number of round trips is minimized (i.e., equals one). Besides, we have shown that the delay of a circuit path is a posynomial function in wire and buffer sizes under the transmission line model, implying that a local optimum is equal to the global optimum. Thus, we can determine the optimal wire and buffer sizes for performance optimization by applying an efficient algorithm, such as the gradient search procedure. Experimental results have shown the effectiveness of simultaneous wire and buffer sizing in performance optimization under the transmission line model.

References

[1] H. B. Bakoglu, *Circuit, Interconnections and Packaging for VLSI*, Addison-Wesley Publishing Company, Inc., 1990.

[2] M. S. Bazaraa, H. D. Sherali, and C. M. Shetty, *Nonlinear Programming: Theory and Algorithms*, John Wiley and Sons, Inc., NY, 1993.

[3] C. P. Chen, Y. P. Chen, and D. F. Wong, "Optimal Wire-Sizing Formula Under the Elmore Delay Model," *Proc. DAC*, pp. 487–490, June 1996.

[4] C. P. Chen, C. C. N. Chu, and D. F. Wong, "Fast and Exact Simultaneous Gate and Wire Sizing by Lagrangian Relaxation," *Proc. ICCAD*, pp. 617–624, Nov. 1998.

[5] C. C. N. Chu and D. F. Wong, "A Polynomial Time Optimal Algorithm for Simultaneous Buffer and Wire Sizing," *Proc. DATE*, pp. 479–485, 1998.

[6] A. Deutsch, Gerard V. Kopcsay, Phillip J. Restle, Howard H. Smith, G. Katopis, Wiren D. Becker, Paul W. Coteus, Christopher W. Surovic, Barry J. Rubin, Richard P. Dunne, Jr., T. Gallo, Keith A. Jenkins, Lewis M. Terman, Robert H. Dennard, George A. Sai-Halasz, Byron L. Krauter, and Daniel R. Knebel, "When are Transmission-Line Effects Important for On-Chip Interconnections?", *IEEE Trans. on Microwave Theory and Techniques*, vol. 45, pp. 1836–1846, Oct. 1997.

[7] R. J. Duffin, E. L. Peterson, and C. Zener, *Geometric Programming: Theory and Application*, John Wiley & Sons, Inc., NY, 1967.

[8] W. C. Elmore, "The Transient Response of Damped Linear Networks with Particular Regard to Wide Band Amplifiers," *J. Applied Physics*, Vol. 19, No. 1, 1948.

[9] Y. Gao and D. F. Wong, "Shaping a VLSI Wire to Minimize Delay Using Transmission Line Model," *Proc. ICCAD*, pp. 611–616, Nov. 1998.

[10] Y. Gao and D. F. Wong "Wire-sizing for Delay Minimization and Ringing Control Using Transmission Line Model," *Proc. DATE*, pp. 512–516, 2000.

[11] Y. I. Ismail and E. G. Friedman, "Effects of Inductance on the Propagation Delay and Repeater Insertion in VLSI Circuits," *IEEE TVLSI*, vol. 8, no. 2, April 2000.

[12] H. R. Jiang, J. Y. Jou, and Y. W. Chang, "Noise-Constrained Performance Optimization by Simultaneous Gate and Wire Sizing Based on Lagrangian Relaxation," *Proc. DAC*, pp. 90–95, June 1999.

[13] J. Lee and E. Shragowitz, "Overshoot and Undershoot Control for Transmission Line Interconnects," *Proc. ECTC*, pp. 879–884, 1999.

[14] T. Lin and L. T. Pileggi, "RC(L) Interconnect Sizing with Second Order Considerations via Posynomial Programming," *Proc. ISPD*, pp. 16–21, April 2001.

[15] F. Moll, M, Roca, A. Rubio, "Inductance in VLSI interconnection modeling," *Proc. of IEE Circuits, Devices and Systems*, vol. 145, issue 3, pp. 175–179, June 1998.

[16] S. G. Nash and A. Sofer, *Linear and Nonlinear Programming*, McGraw-Hill, Inc., 1996.

[17] L. T. Pillage and R. A. Rohrer, "Asymptotic Waveform Evaluation for Timing Analysis," *IEEE TCAD*, Vol. 9, No. 4, pp. 352–366, April 1990.

[18] R. Gupta, L. Pileggi, "Modeling Lossy Transmission Lines Using the Method of Characteristics," *IEEE TCAS-1*, Vol. 43, No. 7, pp. 580–582, July 1996.

[19] Jan M. Rabaey, *Digital Integrated Circuits: A Design Perspective*, Prentice Hall, Inc., 1996.

[20] J. Rebinstein, P. Penfield, Jr., and M. A. Horowitz, "Signal Delay in RC Tree Networks," *IEEE TCAD*, Vol. CAD-2, pp. 202–211, July 1983.

[21] J. S. Roychowdhury, A. R. Newton, and D. O. Pederson, "Algorithms for the transient simulation of lossy interconnect," *IEEE TCAD*, vol. 13, pp. 96–104, Jan. 1994.

[22] K. L. Shepard, D. Sitaram, and Yu Zheng, "Full-chip, three-dimensional, shapes-based RLC extraction," *Proc. ICCAD*, pp. 142–149, 2000.

[23] Semiconductor Industry Association, *International Technology Roadmap for Semiconductors 1999 Edition*, Nov. 1999.

[24] Y. Sugiuchi, B. Katz, and R. A. Rohrer, "Interconnect Optimization using Asymptotic Waveform Evaluation(AWE)," *Proc. MCMC*, pp. 120–125, 1994.

[25] Wayne Wolf, *Modern VLSI Design: Systems on Silicon*, 2nd Editon Prentice Hall, Inc., 1996.

[26] J. S. H. Wang and W. W. M. Dai, "Optimal Design of Self-

Damped Lossy Transmission Lines for Multichip Modules," *Proc. ICCAD*, pp. 594–598, 1994.

[27] T. Xu, E. S. Kuh, and Q. Yu, "A Sensitivity-Based Wiresizing Approach to Interconnect Optimization of Lossy Transmission Line Topologies," *Proc. MCMC*, pp. 117–122, 1996.

[28] Q. Yu and E. S. Kuh, "Exact Moment Matching Model of Transmission Lines and Application to Interconnect Delay Estimation," *IEEE TVLSI*, Vol. 3, No. 2, pp. 311–322, June 1995.

[29] Q. Yu, E. S. Kuh, and T. Xu, "Moment Models of General Transmission Lines with Application to Interconnect Analysis and Optimization," *IEEE TVLSI*, Vol. 4, No. 4, pp. 477–494, Dec. 1996.

[30] Q. Zhu, W. W. M. Dai, and J. G. Xi, "Optimal Sizing of High-Speed Clock Networks Based on Distributed RC and Lossy Transmission Line Models," *Proc. ICCAD*, pp. 628–633, 1993.

[31] Q. Zhu and W. M. Dai, "High-speed clock network sizing optimization based on distributed RC and Lossy RLC interconnect models," *IEEE TCAD*, vol. 15, no 9, pp. 1106–1118, Sep. 1996.

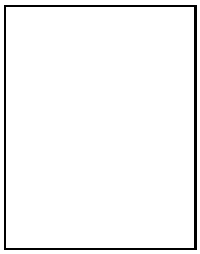

Tai-Chen Chen received the B.S. and M.S. degrees in Computer and Information Science from National Chiao Tung University, Hsinchu, Taiwan, in 1999 and 2001, respectively. He is currently working toward the Ph.D. degree in the Graduate Institute of Electronics Engineering in National Taiwan University. His current research interests include computer-aided design and interconnect optimization for deep submicron technology. Mr. Chen received the Best M.S. Thesis Award from the National Science Council of the Republic of China in 2002.

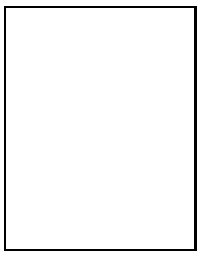

Song-Ra Pan received the B.S. and M.S. degrees in Computer and Information Science from National Chiao Tung University, Taiwan, in 1998 and 2000, respectively. Currently, he is a Ph. D. student in the department of Electronics Engineering , Taiwan. His research interests include foorplan and routing designs in VLSI.

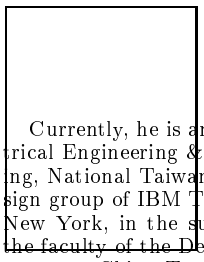

Yao-Wen Chang (S'94–M'96) received the B.S. degree from National Taiwan University in 1988, and the M.S. and the Ph.D. degrees from the University of Texas at Austin in 1993 and 1996, respectively, all in computer science.

Currently, he is an Associate Professor in the Department of Electrical Engineering & the Graduate Institute of Electronics Engineering, National Taiwan University, Taiwan. He was with the VLSI design group of IBM T. J. Watson Research Center, Yorktown Heights, New York, in the summer of 1994. From 1996 to 2001, he was on the faculty of the Department of Computer and Information Science, National Chiao Tung University, Taiwan, where he received an inaugural all-university Excellent Teaching Award (ranked #1 in the Department) in 2000. His research interests lie in physical design automation, architectures, and systems for VLSI and combinatorial optimization.

Dr. Chang received Best Paper Award at the 1995 IEEE International Conference on Computer Design (ICCD-95) for his work on FPGA routing, reviewers' Best Paper nominations at the 2000 ACM/IEEE Design Automation Conference (DAC-2000) for his work on the B*-tree floorplan representation, and Best Paper nomination at the 2002 IEEE/ACM International Conference on Computer-Aided Design (ICCAD-2002) for his work on multilevel routing. He has served on the technical program committees of several international conferences on VLSI design automation. He is a member of IEEE Circuits and Systems Society, ACM, and ACM/SIGDA.